IRRADIATION OF THE MOON BY GALACTIC COSMIC RAYS AND OTHER PARTICLES

James H. Adams, Jr.

E. O. Hulburt Center, Naval Research Laboratory, Washington, DC 20375

Maurice M. Shapiro

Max Planck Institüt für Astrophysik, 8046 Garching bei München, Federal Republic of Germany

Men and sensitive instruments on a lunar base can be profoundly affected by the radiation environment of the Moon. The ionizing radiation incident upon the lunar surface is comprised of the galactic cosmic rays (GCR) and energetic particles accelerated in the solar neighborhood. The latter consist mainly of solar energetic particles (SEP) from flares and of other particles energized in the heliosphere. The cosmic radiation bombarding the Moon consists overwhelmingly of relativistic and near-relativistic atomic nuclei ranging in energy from 10^8–10^{20} eV, approximately 98.6% of which consists of hydrogen and helium. The remainder spans the rest of the periodic table, with conspicuous peaks in abundance at C, O, Ne, Mg, Si, and Fe. The GCR composition is roughly similar to that of the sun, with some notable differences. Differential energy spectra and composition of cosmic rays as well as the intensities, composition, and the spectra of SEP and particles accelerated in the heliosphere are reviewed. We also summarize the analytic models developed by the Naval Research Laboratory (NRL) group to describe the energy spectra and elemental compositions of the various components.

THE LUNAR RADIATION ENVIRONMENT

The Moon is constantly bombarded by galactic cosmic rays (GCR). Figure 1 (from Simpson, 1983) shows a sampling of the data available on the differential energy spectra of the most prominent particle types in galactic cosmic rays. The intensity of this highly penetrating particle radiation varies in response to solar activity. In a way that is not yet fully understood (Fillius and Axford, 1985), the out-flowing solar wind modulates the cosmic ray intensity so that it is anti-correlated with the general level of solar activity. This causes the average intensity of cosmic rays with energies greater than 10 MeV/amu to increase 2.5 times from the maximum to the minimum of the 11-year solar activity cycle. Low energy cosmic rays are affected more strongly than the higher energy ones. Figure 2 (from Simpson, 1983) compares the elemental compositions of galactic cosmic rays and the solar system, normalized at silicon. The two compositions are comparable for the most abundant elements. The odd elements, in general, and Li, Be, B, F, Sc, Ti, V, Cr, and Mn, in particular, are overabundant in galactic cosmic rays. This difference is the result of the propagation of galactic cosmic rays through approximately 7 g/cm^2 of interstellar gas, on average, before reaching Earth (Shapiro and Silberberg, 1970).

During periods of minimum solar activity, additional components can be observed at low energy. One component is constantly present. This component, discovered by Garcia-

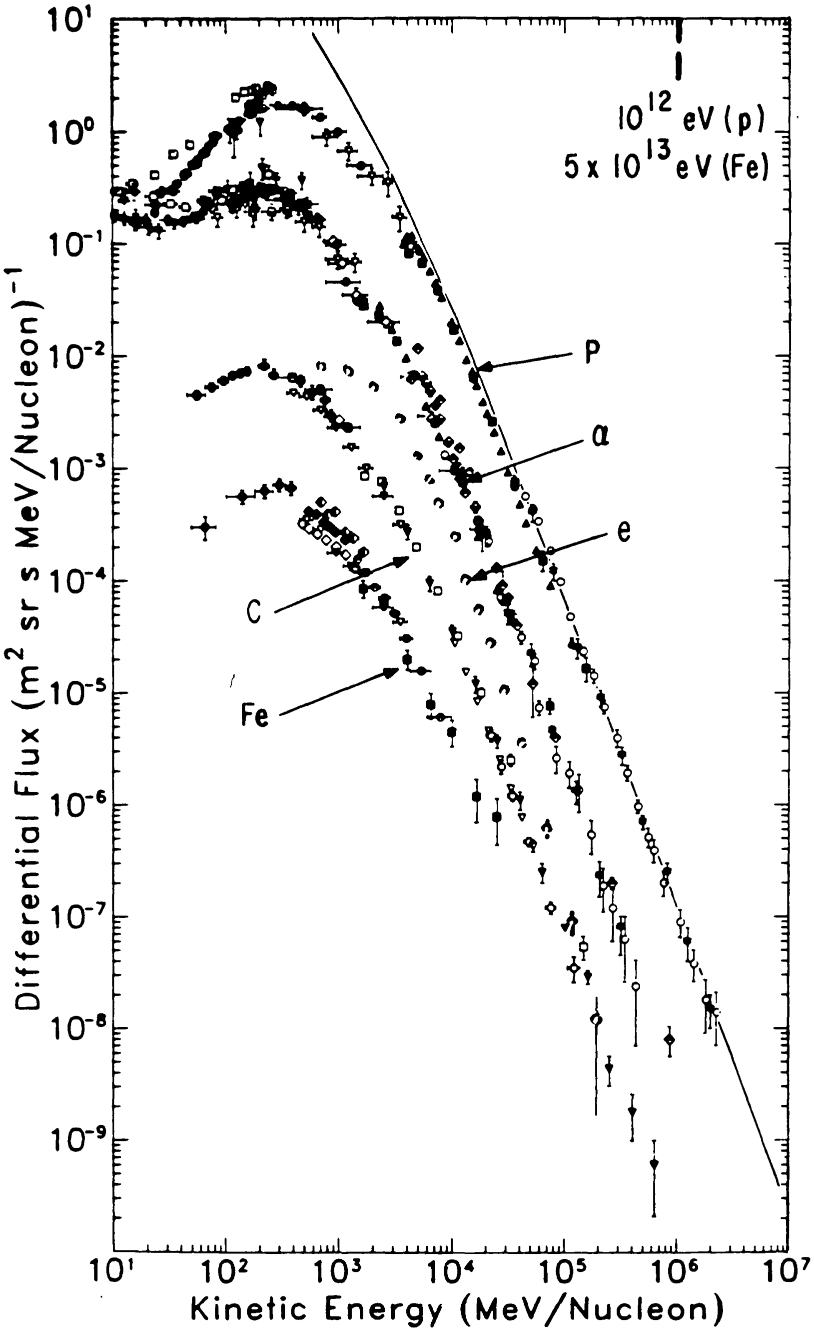

Figure 1. The differential energy spectra for the elements (from the top) hydrogen (P), helium (α), carbon (C), and iron (Fe). Also shown is the electron spectrum (labeled e). The solid curve shows the hydrogen spectrum extrapolated to interstellar space by unfolding the effects of modulation. The turn-up of the helium spectrum below about 60 MeV/nucleon is due to the contribution of the anomalous component of helium. This figure was taken from Simpson (1983).

Munoz *et al.* (1973), is called the anomalous component because of its unusual nature. Figure 3 shows the spectra of H, He, C, and O in the interplanetary medium. The anomalous component is the broad peak in the low energy oxygen spectrum and the absence of a dip in the helium spectrum at 10 MeV/amu that causes the helium flux to exceed the hydrogen flux in this energy range. A second component is sometimes accelerated in regions where fast and slow moving solar wind streams collide (Gloeckler, 1979). These co-rotating energetic particles will sometimes cause modest increases in the 1–10 MeV/

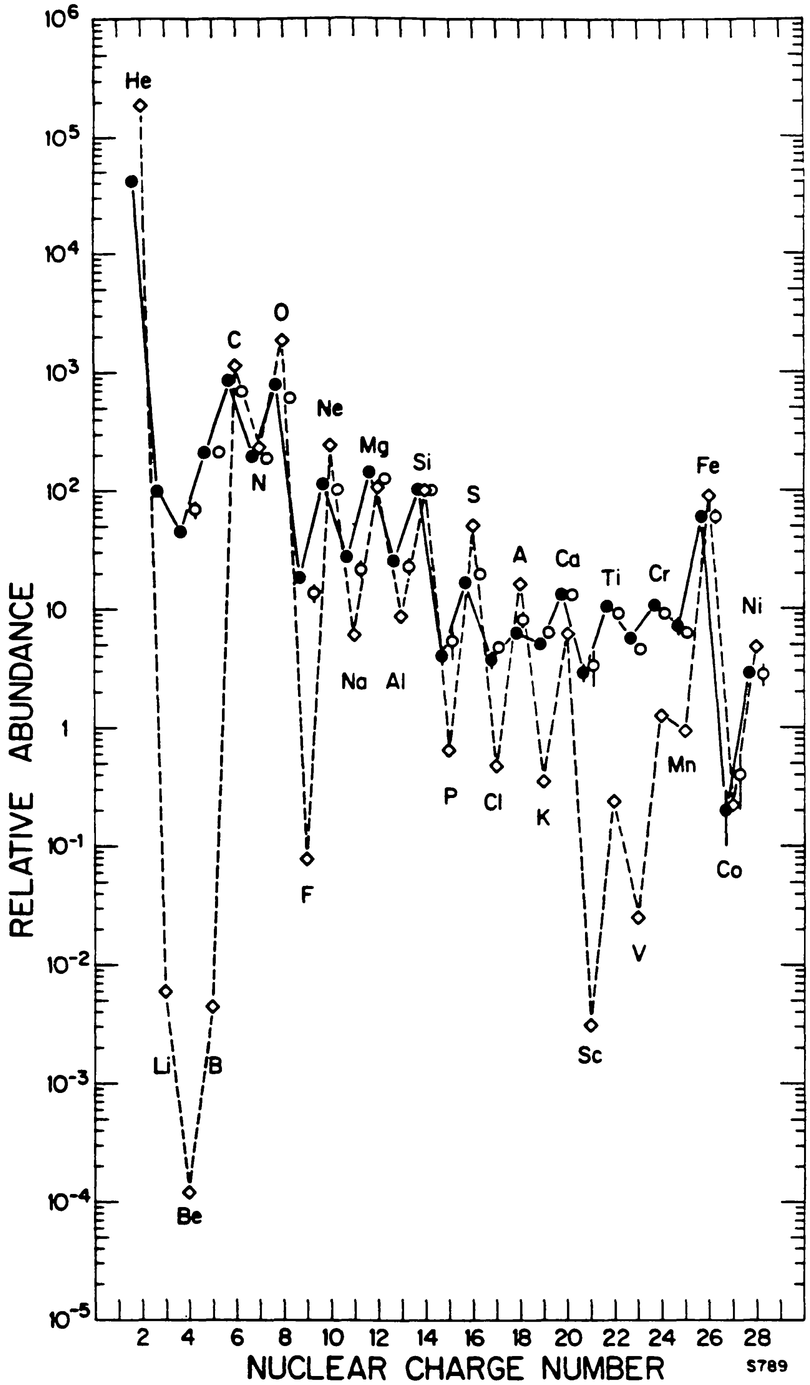

Figure 2. The cosmic ray element abundances (He-Ni) measured at Earth compared to the solar system abundances. The two abundances are normalized at silicon. The diamonds represent the solar system abundances, while the open circles are cosmic ray measurements at high energies in the 1000–2000 MeV/nucleon range. Hydrogen, not shown, is about 20 times more abundant in the solar system than in cosmic rays, using silicon as the normalization. This figure was taken from Simpson (1983).

amu hydrogen and helium fluxes bombarding the Moon. Because these components exceed the cosmic ray background only at low energies, their contribution to the total particle intensity bombarding the Moon is small.

Occasionally there are major increases in the radiation intensity at the Moon due to solar energetic particle (SEP) events. These events last from hours to days and range in size from the limit of detection to an intensity more than 70,000 times that of galactic

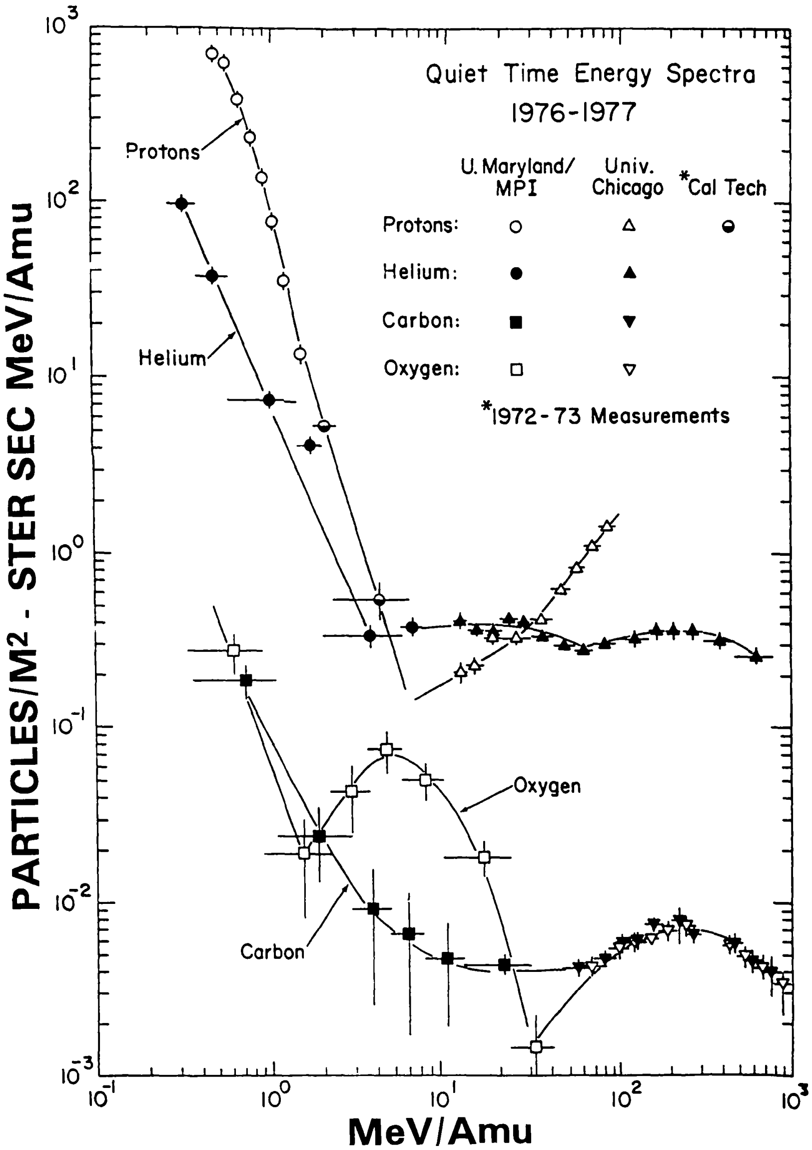

Figure 3. Differential energy spectra of hydrogen, helium, carbon, and oxygen observed in the interplanetary medium near the Earth during the solar minimum in 1976–77 during quiet times. The anomalous cosmic ray component appears between 2 and 30 MeV/nucleon and is characterized by the large overabundance of helium and oxygen compared to hydrogen (protons) and carbon, respectively. This figure was taken from Gloeckler (1979).

cosmic rays. So large are the largest of these events that they determine the particle fluence at the lunar surface over a solar cycle. It is usually true that half the particles to strike the Moon in an 11-year solar cycle arrive in less than a day and are the result of one, or at most a few, large SEP events. This striking feature will make a flare watch an important part of any future lunar expedition, as it was during the Apollo program.

McGuire *et al.* (1983) show the record of SEP events for the last three solar cycles. Their results are reproduced in Fig. 4. As this figure shows, the frequency of SEP events varies with the overall level of solar activity as gauged by the smoothed Zurich sunspot number. McGuire *et al.* find the solar-cycle-averaged hydrogen fluxes above 10 MeV for cycles 19, 20, and 21 are 378, 93, and 65 particles/cm^2 s. These fluxes are 132, 33, and 23 times larger than the solar-cycle-averaged galactic cosmic ray hydrogen flux, respectively.

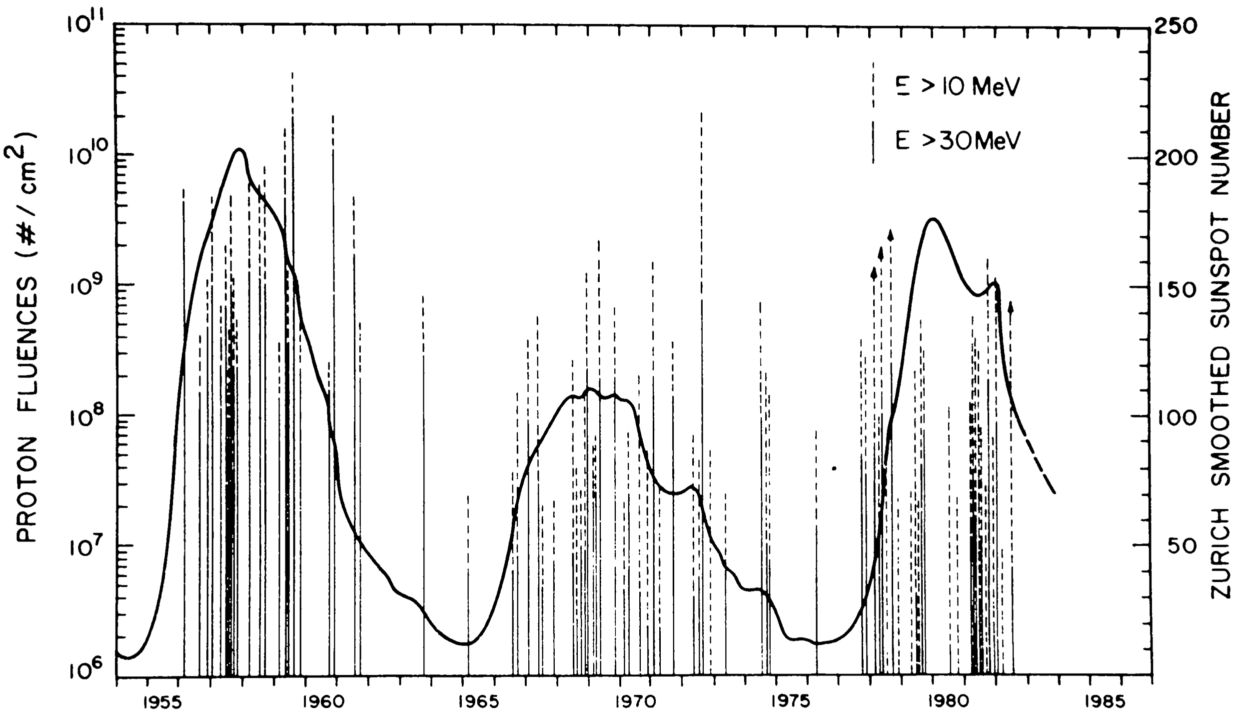

Figure 4. Hydrogen fluences above 10 and 30 MeV in Solar Energetic Particle Events during solar cycles 19, 20, and 21. The solid curve represents Zurich smoothed sunspot numbers. This figure was taken from McGuire et al. (1983).

The spectra of SEP events are much softer than the galactic cosmic ray spectrum. Even during the peak intensity of most SEP events, galactic cosmic rays are the principal source of particles above a few hundred MeV/amu. The largest observed flares have, at their peak, dominated the flux up to 10,000 MeV/amu.

The elemental composition of SEP events is very similar to the solar system composition (shown in Fig. 2) on average but can be highly variable from one event to the next. The composition even varies with particle energy in individual events (Chenette and Dietrich, 1984). SEP events that are enriched in one heavy ion tend to be enriched in the others as well. Dietrich and Simpson (1978) have shown that this systematic enrichment increases strongly with atomic number.

THE NRL CREME MODEL

A procedure has been developed at Naval Research Laboratory to characterize cosmic ray effects on microelectronics (CREME) used in spacecraft and aircraft (see Adams *et al.*, 1981; Adams *et al.*, 1983; and Tsao *et al.*, 1984). This procedure relies on a detailed numerical model of the near-Earth particle environment (Adams *et al.*, 1981), which is directly applicable to characterizing the radiation environment on the Moon. A set of formulas describes the differential energy spectra of each of the elements in galactic cosmic rays and how these spectra are modified by the contributions from the anomalous

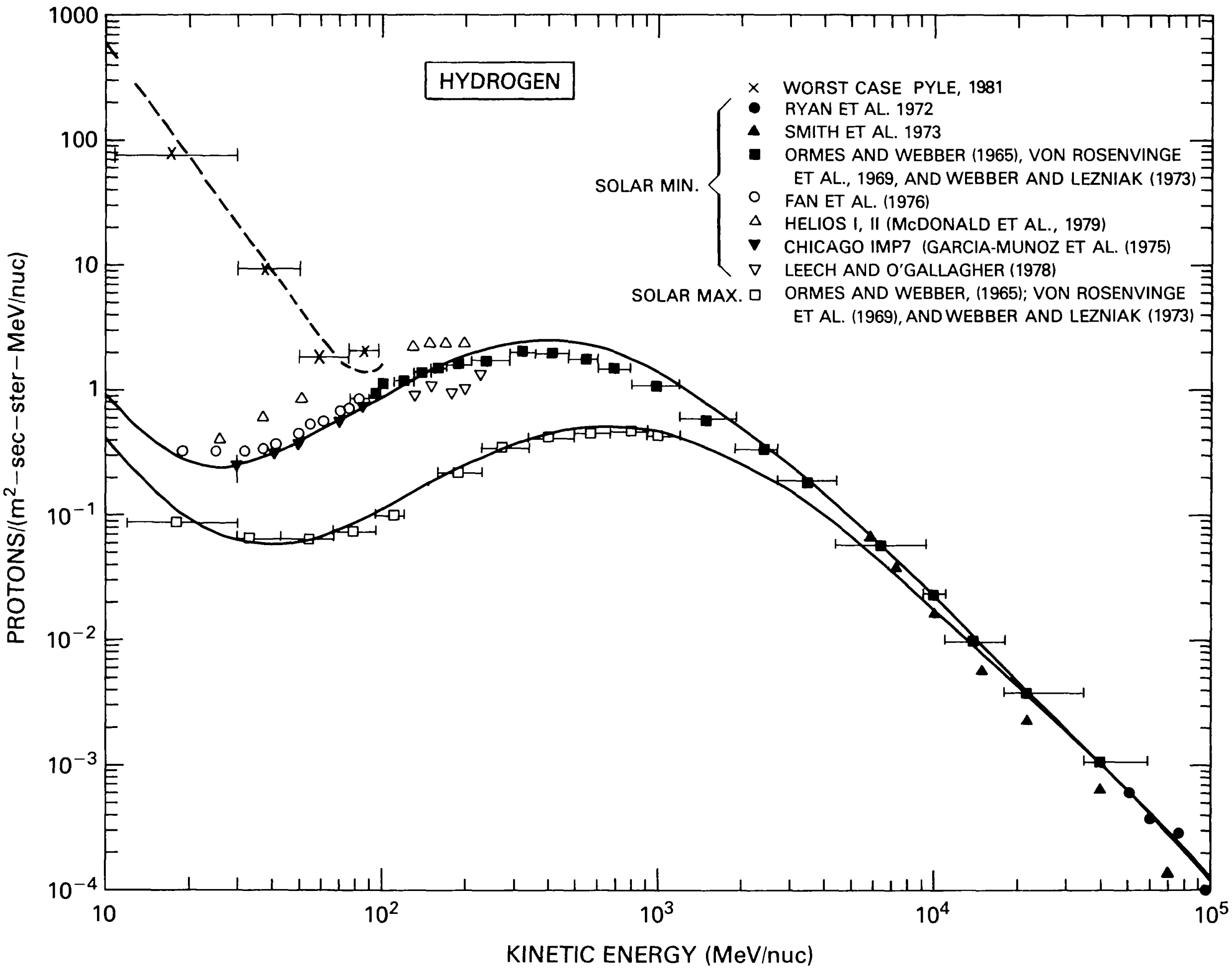

Figure 5. Hydrogen differential energy spectra (taken from Adams et al., 1981). The data are selected for the extremes of solar maximum and solar minimum. The solid curves are from the formulas to fit the cosmic ray spectra for solar minimum (upper curve) and solar maximum (lower curve). The dashed curve is from a formula constructed to give instantaneous flux levels so high at each energy that they are exceeded only 10% of the time.

component, co-rotating energetic particle streams, and from small flares. The model also contains formulas for the differential energy spectra of each of the elements in SEP events and formulas for calculating the probability of occurrence of such events.

Galactic cosmic rays were modeled by using all the available data to determine the shapes of the differential energy spectra of hydrogen, helium, and iron at the extremes of solar maximum and solar minimum. Figures 5, 6, and 7 show how the model (solid lines) fit the data for hydrogen, helium, and iron, respectively. The model spectra are for the extremes of solar maximum and minimum. Intermediate cases are interpolated with a sinusoidal solar modulation factor of sin[2 $(t\text{-}t_0)/10.9$ years)], where $t_0 = 1950.6$. The other elemental spectra are obtained by multiplying either the helium or the iron spectrum by a constant or, in some cases, energy-dependent scale factor. By comparing

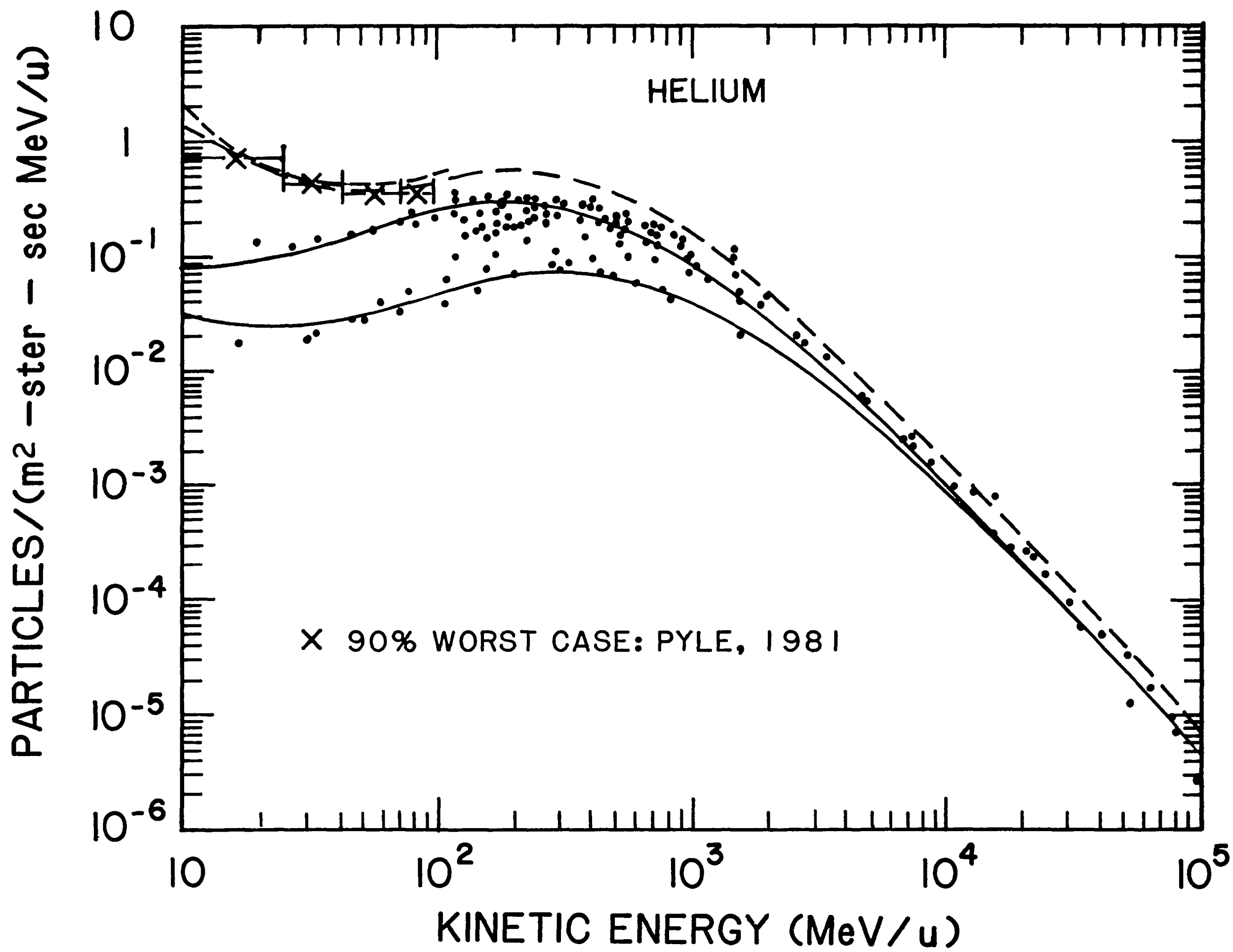

Figure 6. Helium differential energy spectra (taken from Adams et al., 1981). The solid curves are from the formulas to fit the cosmic ray spectra for solar minimum (upper curve) and solar maximum (lower curve). The dashed curve is from a formula constructed to give instantaneous flux levels so high at each energy that they are exceeded only 10% of the time.

this model with recent data, we find that it seems to predict the absolute cosmic ray flux to within a factor of two. The relative abundances are accurate to about 20%.

The contributions at low energies from co-rotating particle streams and small SEP events were accounted for along with the overall uncertainty by the 90% worst-case model. This model is shown as the dashed curves in Figs. 5–7. The contributions of the anomalous component to the helium, nitrogen, and oxygen spectra are modeled by Adams *et al.* (1981), who show how these may be combined with the cosmic ray model spectra to account for the contributions of the anomalous component at low energies.

Following the scheme of King (1974), Adams *et al.* (1981) divided all the large SEP events into ordinary large flares and anomalously large flares. A formula was fitted to the means of the log-normal distributions of the integral SEP flux above several energy thresholds and then differentiated to obtain the mean hydrogen differential energy spectrum for ordinary large SEP events. This procedure was repeated using values 1.28 standard

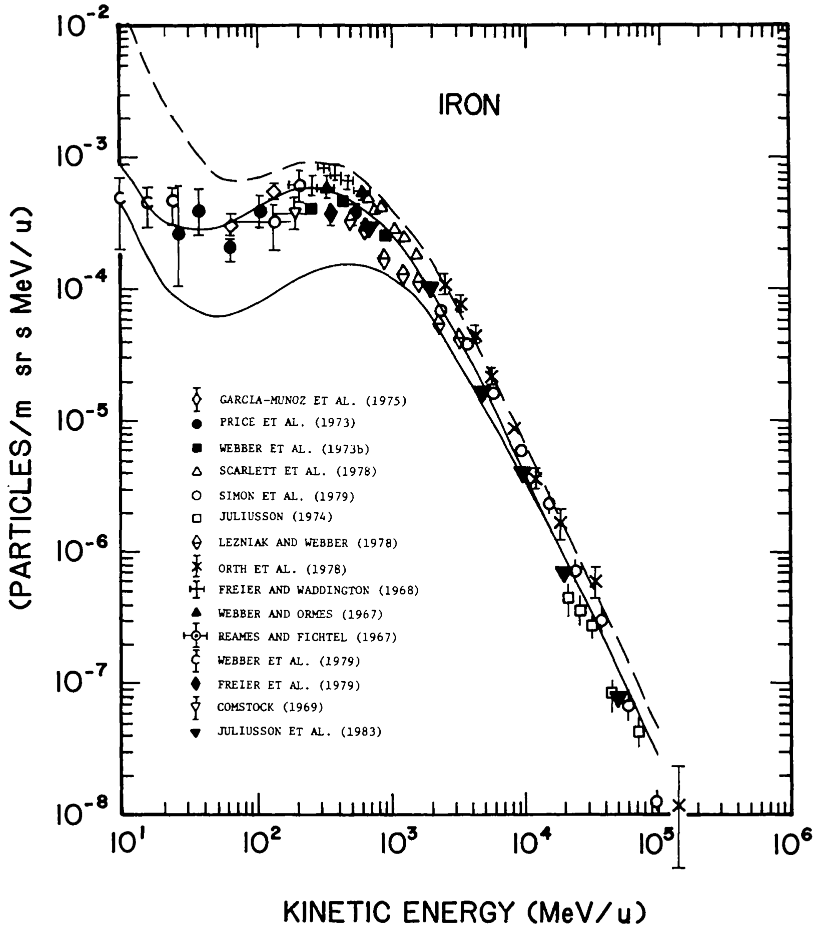

Figure 7. Iron differential energy spectra (taken from Adams et al., 1981). The solid curves are from the formulas to fit the cosmic ray spectra for solar minimum (upper curve) and solar maximum (lower curve). The dashed curve is from a formula constructed to give instantaneous flux levels so high at each energy that they are exceeded only 10% of the time. This dashed curve has been constructed by comparison with helium, since iron data to establish this curve directly are lacking.

deviations above the means of the log-normal distributions to obtain a spectrum for the 90% worst-case SEP event. Again, following King (1974), the SEP event of August 4, 1972 was used as the model for anomalously large events. These three model hydrogen spectra are shown in Fig. 8.

The composition of the SEP events is given by Adams *et al.* (1981) as elemental abundances relative to hydrogen for both the mean heavy ion composition and a 90% worst-case enrichment in the heavy elements. These two compositions, shown in Fig. 9, indicate the degree of variability in the SEP composition. Burrell distribution formulas are also provided by Adams *et al.* (1981) to calculate the probability of an SEP event during any time period.

RADIATION EFFECTS ON THE MOON

If a large permanent base is established on the Moon, the 5 rem/y exposure limit for Earth-based radiation workers might be a more appropriate standard for radiation protection. As Silberberg *et al.* (1985) show, adherence to this standard would make it necessary to bury a lunar habitat beneath several meters of lunar regolith and limit human activity on the lunar surface to "regular working hours," *i.e.*, about 1800 hours

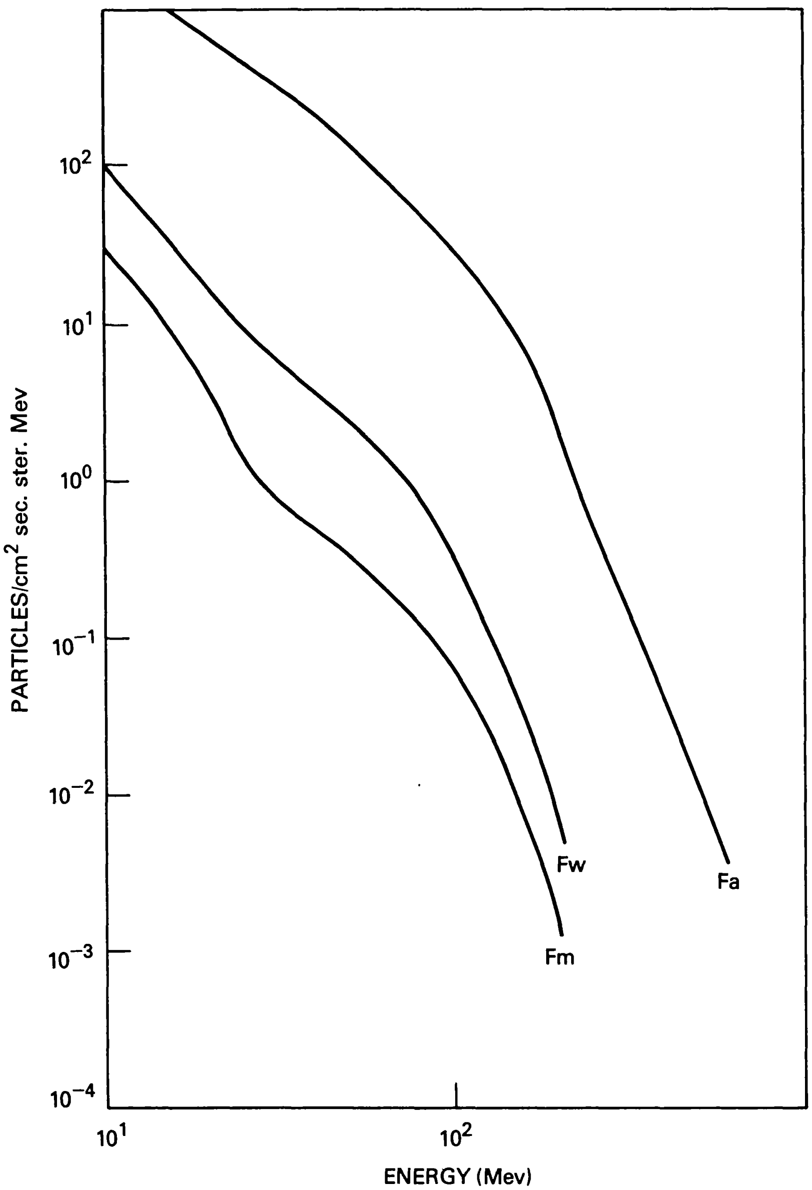

Figure 8. Hydrogen differential energy spectra (taken from Adams et al., 1981). These spectra are for the peak intensities of three model solar energetic particle (SEP) events. The curve labeled Fm is for the mean large SEP event (using the definition of King, 1974). A second model SEP event (curve Fw) has been constructed such that only one SEP event in 10 will have a peak intensity, at any energy, that is greater than predicted by this event. These two curves may be compared to get a feel for the range of flare sizes. The Fa curve is modeled after the peak of the SEP event of August 4, 1972. This is one of the most severe SEP events ever observed.

per year inside an enclosed vehicle. Extravehicular activity would have to be restricted. Even then, people working on the surface would have to remain near the habitat so that they could rush to shelter in case of a large SEP event. Long expeditions across the lunar surface would be risky unless shelters could be constructed a few hours travel time apart, or a means could be provided to quickly rescue the expedition and return its members to the safety of the buried lunar habitat.

The lunar radiation environment affects not only people, but electronic systems as well. It has long been known that electronic components are affected by the total radiation dose they have accumulated. This radiation damage produces changes in conductivity or shifts in device thresholds that cause a malfunction of the electronic circuit. Electronic components have been developed that can tolerate very large total doses, so that it is

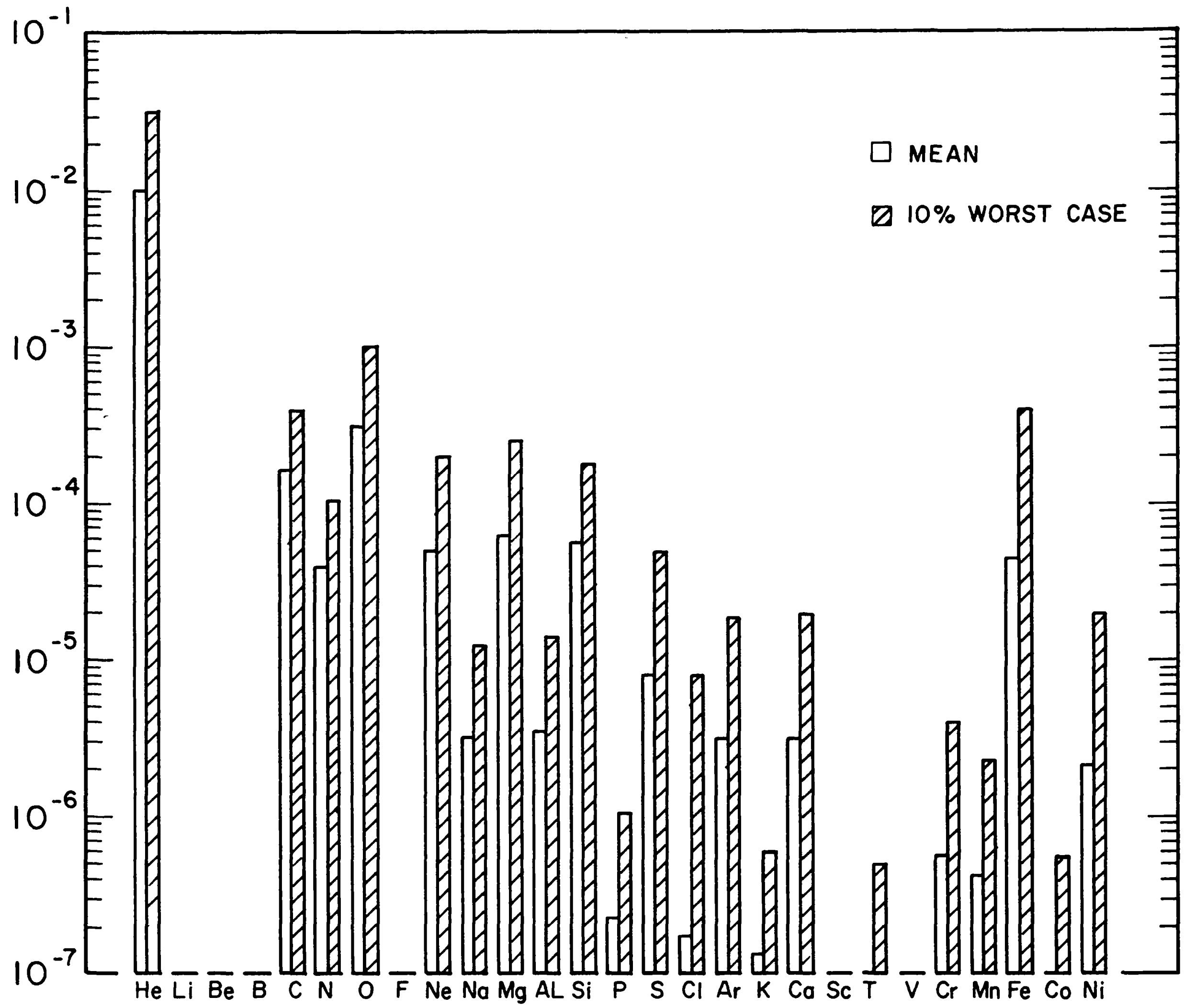

Figure 9. Elemental composition of Solar Energetic Particle (SEP) events (taken from Adams and Gelman, 1984). The mean SEP composition, normalized to hydrogen, is compared with a composition (10% worst case) constructed so that only one SEP event in 10 will be richer in any heavy ion. Comparing the two compositions, we can see that the iron to hydrogen ratio in a heavy ion-rich event may exceed the oxygen to hydrogen ratio for a typical event.

possible to design electronic systems for use on the Moon with operational lifetimes in excess of 10 years.

Recently, it has been discovered that single, intensely ionizing particles can produce a burst of hole-electron pairs so large that the resulting charge or current can change the logic state of a modern digital microcircuit (Adams *et al.*, 1981, 1983; Tsao *et al.*, 1984). This change of state damages not the electronic circuitry but the information stored in it. These events are therefore called "soft upsets."

The operational impact of a soft upset depends on the microcircuit affected. If the microcircuit is in the program memory of a computer, the program will no longer be operable and must be reloaded. If it is in the microprocessor's address registers or program counter, the actions the computer takes will be unpredictable. Soft upsets in control circuitry can also result in unplanned events such as thruster firings. It is clear that a single soft upset could cause the loss of equipment and personnel. Unlike total dose sensitivity, soft upset susceptibility is a fundamental feature of modern large-scale integrated circuits. It appears unlikely that such compact circuits can be made immune to soft upsets. The problem has been attacked at the system level instead, with redundancy, fault tolerance, and software checking. These methods reduce, but do not eliminate, the risks posed by soft upsets.

COSMIC RAY EXPERIMENTS FOR A LUNAR BASE

The Moon offers the possibility of doing cosmic ray experiments that would be difficult to carry out in Earth orbit. On the Moon, lunar regolith can be used for the massive absorbers needed in some large detector systems. The Moon also offers a site for the construction of large detector arrays beyond the protection of the Earth's magnetic field. Two possible experiments are discussed here.

The energy spectrum of cosmic rays has been measured directly up to 1 TeV/nuc (Watson, 1975). The only direct measurement above this energy is due to Grigorov *et al.* (1971). Therefore, most of what is known about cosmic rays above 1 TeV/nuc is based on indirect measurements that provide only total particle energy as determined from the shower of secondary particles produced in the atmosphere by an incident cosmic ray. Direct measurements at these higher energies will make it possible to establish the particle's charge and, hence, its velocity and magnetic rigidity. The latter quantity can be compared with the available data on galactic magnetic fields to determine whether the particles at these high energies could have come from our galaxy or must be extra-galactic.

The best device for measuring these high energies directly is an ionization calorimeter of the type developed at Goddard Space Flight Center (Balasubrahmanyan and Ormes, 1973). One square meter calorimeters could be constructed on the lunar surface, using regolith to replace the heavy iron plates in the Goddard design. A single calorimeter of this size would detect events up to 10,000 TeV/nuc in the first year of operation, and 100 such units could extend the spectrum to the interesting region above 100,000 TeV/nuc in a few years. A secondary benefit of such an experiment might be the opportunity to study elementary particle interactions at energies well above those achieved at accelerators. Such investigations could lead to new discoveries pointing the way for new particle physics experiments on Earth.

Experiments employing NASA's Long Duration Exposure Facility, presently underway and planned for the near future, are expected to establish the flux of actinide nuclei in galactic cosmic rays. This will tell us whether cosmic ray source material resembles the interstellar medium or is enriched in nuclei synthesized by the rapid neutron capture (r-) process. Whatever the nucleosynthetic origin of cosmic rays may turn out to be, these near-term experiments will not tell us how much time has elapsed since cosmic ray material was synthesized. To answer this question, it will be necessary to measure the abundances of the individual actinide nuclei. The relative abundances of Th, U, Np, Pu, and Cm tell us the elapsed time since the nucleosynthesis of cosmic rays in the range of 10^7 to 10^9 years. To measure them would require 2000 m^2 ster. years of collecting power. As suggested by Waddington (personal communication, 1984), this could be provided by a cylindrical array of scintillators 10 m in diameter and 10 m high. Such an apparatus could be placed on the lunar surface, and it would collect a suitable sample of events in less than 5 years. The array would use time of flight across the cylinder to measure velocity, so that the scintillator signals could be corrected for velocity to obtain the particle's charge.

CONCLUSIONS

The ionizing radiation environment on the lunar surface poses a hazard to men and sensitive instruments. Measures to protect crews from this environment can be expected to influence the design of lunar bases and the planning of lunar surface activities.

The lunar surface offers a site for large cosmic ray experiments to measure the abundances of rare elements and extremely high energy particles. The experiments that are possible on the Moon will provide new information on the origin of cosmic rays and possibly on the interaction of ultra-high energy particles with matter.

REFERENCES

Adams J. H. and Gelman A. (1984) The effects of solar flares on single event upset rates. *IEEE Trans. Nucl. Sci., NS-31*, 1212–1216.

Adams J. H., Silberberg R., and Tsao C. H. (1981) Cosmic ray effects on microelectronics, Part I: *The Near-earth Particle Environment.* NRL Memorandum Report 4506, Naval Research Laboratory, Washington, DC. 92 pp.

Adams J. H., Letaw J. R., and Smart D. F. (1983) *Cosmic Ray Effects on Microelectronics, Part II: The Geomagnetic Cutoff Effects.* NRL Memorandum Report 5099, Naval Research Laboratory, Washington, DC. 45 pp.

Balasubrahmanyan V. K. and Ormes J. F. (1973) Results on the energy dependence of cosmic-ray charge composition. *Ap. J., 186*, 109–122.

Chenette D. L. and Dietrich W. F. (1984) The solar flare heavy ion environment for single event upsets: A summary of observations over the last solar cycle, 1973–1983. *IEEE Trans. Nucl. Sci., NS-31*, 1217–1222.

Dietrich W. F. and Simpson J. A. (1978) Preferential enhancements of the solar flare-accelerated nuclei carbon to zinc from ~20–300 MeV nucleon. *Ap. J., 225*, L41–L45.

Fillius W. and Axford I. (1985) Large scale solar modulation of $\lesssim$500 MeV/Nucleon galactic cosmic rays seen from 1 to 30 AU. *J. Geophys. Res., 90*, 517–520.

Garcia-Munoz M., Mason G. M., and Simpson J. A. (1973) A new test for solar modulation theory: The 1972 May-July low-energy galactic cosmic-ray proton and helium spectra. *Ap. J., 182*, L81–L84.

Gloeckler G. (1979) Compositions of energetic particles populations in interplanetary space. *Rev. Geophys. Space Phys., 17*, 569–582.

Grigorov N. L., Gubin Yu V., Rapaport I. D., Savenko I. A., Akimov V. V., Nesterov V. E., and Yakovlev B. M. (1971) Energy spectrum of primary cosmic rays in the 10^{11}–10^{15} eV energy range according to the data of proton-IV measurements. *Proc. 12th Intl. Cosmic Ray Conf., 5*, pp. 1746–1751.

King J. H. (1974) Solar proton fluences for 1977–1983 space missions. *J. Spacecraft Rockets, 11*, 401–408.

McGuire R. E., Goswami J. N., Jha R., Lal D., and Reedy R. C. (1983) Solar flare fluences during solar cycles 19, 20, and 21. *Proc. 18th Intl. Cosmic Ray Conf., 44*, pp. 66–69.

Shapiro M. M. and Silberberg R. (1970) Heavy cosmic ray nuclei. *Ann. Rev. Nucl. Sci., 20*, 323.

Silberberg R., Tsao C. H., Adams J. H. Jr., and Letaw J. R. (1984) Radiation doses and LET distributions of cosmic rays. *Rad. Res., 98*, 209–226.

Silberberg R., Tsao C. H., Adams J. H. Jr., Hulburt E. O., and Letaw J. R. (1985) Radiation transport of cosmic ray nuclei in lunar material and radiation doses (abstract). This volume.

Simpson J. A. (1983) Elemental and isotopic compositions of the galactic cosmic rays. *Ann. Rev. Nucl. Part. Sci., 33*, 323–381.

Tsao C. H., Silberberg R., Adams J. H. Jr., and Letaw J. R. (1984) Cosmic Ray Effects on Microelectronics, Part III: Propagation of Cosmic Rays in the Atmosphere. NRL Memorandum Report 5402, Naval Research Laboratory, Washington, D.C. 87 pp.

Watson A. A. (1975) Energy spectrum and mass composition of cosmic ray nuclei from 10^{12} to 10^{20} eV. In *Origin of Cosmic Rays* (J. L. Osborne and A. W. Wolfendale, eds.), pp. 61–96. Reidel, Dordrecht.